Since January 2020 Elsevier has created a COVID-19 resource centre with free information in English and Mandarin on the novel coronavirus COVID-19. The COVID-19 resource centre is hosted on Elsevier Connect, the company's public news and information website.

Molecular and Cellular Probes 43 (2019) 20–28

Contents lists available at ScienceDirect

Molecular and Cellular Probes

journal homepage: www.elsevier.com/locate/ymcpr

Multiplex SYBR Green and duplex TaqMan real-time PCR assays for the detection of *Photorhabdus* Insect-Related (Pir) toxin genes *pir*A and *pir*B

Roberto Cruz-Flores, Hung Nam Mai, Arun K. Dhar*

Aquaculture Pathology Laboratory, School of Animal and Comparative Biomedical Sciences, The University of Arizona, AZ. 85721, USA

ARTICLE INFO

Keywords:
Acute hepatopancreatic necrosis disease
Early mortality syndrome
Multiplex real-time PCR
SYBR Green
TaqMan
Pathogen detection

ABSTRACT

Acute hepatopancreatic necrosis disease (AHPND), also known as Early mortality syndrome (EMS), is a recently emerged lethal disease that has caused major economic losses in shrimp aquaculture. The etiologic agents are *Vibrio* spp. that carry *Photorhabdus* Insect-Related (Pir) toxin genes *pir*A and *pir*B. A multiplex SYBR Green real-time PCR was developed that detects *pir*A, *pir*B, and two internal control genes, the shrimp 18S rRNA and the bacterial 16S rRNA genes in a single reaction. The *pir*B primers amplify the 3'-end of the *pir*B gene allowing the detection of *Vibrio* spp. mutants that contain a complete deletion of *pir*A and the partial deletion of *pir*B. The assay also detects mutants that contain the entire *pir*A gene and the deletion of the *pir*B gene. Since both toxin genes are needed for disease development, this assays can distinguish between pathogenic strains of *Vibrio* spp. that cause AHPND in shrimp and mutants that do not cause disease. The amplicons for *pir*A, *pir*B, 18S rRNA and 16S rRNA showed easily distinguishable melting temperatures of 78.21 ± 0.18, 75.20 ± 0.20, 82.28 ± 0.34 and 85.41 ± 0.21 °C respectively. Additionally, a duplex real-time PCR assay was carried out by designing TaqMan probes for the *pir*A and *pir*B primers. The diagnostic sensitivity and specificity was compared between the SYBR Green and TaqMan assays. Both assays showed similar sensitivity with a limit of detection being 10 copies for *pir*A and *pir*B, and neither assays showed any cross reaction with other known bacterial and viral pathogens in shrimp. The high sensitivity of both assays make them suitable for the detection of low copies of the *pir*A and *pir*B genes in AHPND causing *Vibrio* spp. as well as for detecting non-pathogenic mutants.

1. Introduction

Acute hepatopancreatic necrosis disease (AHPND, initially referenced to as early mortality syndrome, EMS) is a deadly shrimp disease caused by particular *Vibrio* spp. [1–3]. The disease first emerged in China in 2009 and has rapidly spread throughout Southeast Asia to Vietnam, Malaysia, Thailand and reached Mexico in Latin America in 2013 [1,4]. The impact of AHPND in shrimp farming at a global scale has been catastrophic with an estimated global loss of $1 billion per year [5].

The etiologic agent of AHPND was shown to be a specific strain of *Vibrio parahaemolyticus* that carries the *pir*A and *pir*B genes homologous to the Pir (*Photorhabdus* insect-related) binary toxin of entomopathogenic bacteria [1,3]. Since the initial report, several other *Vibrio* species including *V. owensii* [6], *V. campbelli* [7], *V. harveyi* [8] and *Vibrio punensis* [9] have been reported that cause AHPND. More recently, a non-*Vibrio* bacterium, *Micrococcus luteus,* has been found that contains the *pir*A and *pir*B genes [10].

The pathogenic *Vibrio* spp. harbor a large plasmid that ranges from 69 to 74 kb, on average of 33 copies per cell, and contains *Photorhabdus* Insect-Related (Pir) toxin genes *pir*A and *pir*B [3,11,12]. The binary toxin *pir*AB has been confirmed to be the etiological agent for AHPND [11]. To date, two conventional PCR based methods have been reported to detect both toxins genes *pir*A and *pir*B, a duplex conventional PCR reported by Han et al. [3] and a two-tube nested AP4 PCR developed by Dangtip et al. [13]. However, the two-tube nested AP4 PCR cannot detect deletion mutants that have only one gene *pir*A or *pir*B. A qPCR assay that detects *pir*A but does not detect mutants with the deletion of *pir*B has been reported [14]. The detection of both types of mutants is fundamental for the study of plasmid transmission dynamics and for recording the presence of the virulence plasmid since a recent study [2] suggests that the *pir*A and *pir*B genes may be lost or acquired by horizontal gene transfer via transposition or homologous recombination. In fact, the genome of a mutant strain of *V. parahaemolyticus* has been published that lacks the entire *pir*A gene and has a partial deletion of the 5′-end of the *pir*B gene [15]. In this study, we report a multiplex SYBR Green real-time PCR that detects the *pir*A and *pir*B toxin genes, and two internal control genes, the shrimp 18S rRNA and the bacterial

* Corresponding author.
E-mail address: adhar@email.arizona.edu (A.K. Dhar).

https://doi.org/10.1016/j.mcp.2018.12.004
Received 7 November 2018; Received in revised form 17 December 2018; Accepted 17 December 2018
Available online 18 December 2018
0890-8508/

Table 1
A list of primers that were used for the amplification of *pir*A and *pir*B toxin genes. For each primer, the nucleotide sequence, the Tm, the amplicon size and the location on the virulence plasmid in the reference strain *V. parahaemolyticus* A3 (GenBank accession: KM067908.1) are shown.

Primer Set	Primer pair	Primer sequence (5′ to 3′)	Primer Tm	Product size (bp)	Location in the virulence plasmid of reference strain *Vibrio parahaemolyticus* A3
Set 1	*pir*A F1	TGAAACTGACTATTCTCACGATTG	57	80	17,218 - > 17,241
	*pir*A R1	TGATAGGTGTATGTTTGCTGTC	56.2	80	17,297 - > 17,276
	*pir*B F1	TCACGGCTTTGAACATATGC	56.8	149	18,268 - > 18,287
	*pir*B R1	CATCTTCCGTACCTGTAGCA	56.8	149	18,416 - > 18,397
Set 2	*pir*A F2	AACTGACTATTCTCACGATTGGACT	59.8	101	17,221 - > 17,245
	*pir*A R2	CTACACTACGACCGACTTCCG	59.9	101	17,321 - > 17,301
	*pir*B F2	TTGGGGAACGTCGAAATCGT	60	216	18,447 - > 18,466
	*pir*B R2	TTGCTTCAGGTCCATTGGCA	60.2	216	18,662 - > 18,643
Set 3	*pir*A F3	ACTGTCGAACCAAACGGAGG	60.3	165	17,243 - > 17,262
	*pir*A R3	TTTAGCCACTTTCCAGCCGC	61.2	165	17,407 - > 17,388
	*pir*B F3	TTGCCAATGGACCTGAAGCA	60.2	94	18,642 - > 18,661
	*pir*B R3	ACACTTGGCTTGCCTGAGTT	60.1	94	18,735 - > 18,716

16S rRNA. Furthermore, we report a duplex TaqMan PCR that also detects *pir*A and *pir*B simultaneously. These assays will greatly aid in the detection and monitoring of low quantities of AHPND causing *Vibrio* spp. and mutant strains containing either *pir*A or *pir*B.

2. Methods

2.1. Primer design

Three different primer pairs were designed with Geneious R11 [16] to detect the *pir*A and *pir*B toxin genes (Table 1). The primers for the *pir*B were designed to amplify the 3'-end of the *pir*B gene allowing the detection of *Vibrio* spp. that have a partial deletion of this gene (Fig. 1). The genes used as internal controls for shrimp and bacteria were β-Actin, Elongation factor1-alpha, Glyceroldehyde-3 phosphate dehydrogenase, 18S rRNA, and 16S rRNA (Table 2).

2.2. Multiplex SYBR Green real-time PCR

Multiplex SYBR Green real-time PCR was performed using a StepOnePlus PCR system (Applied Biosystems ™). Each assay was carried out in a total volume of 20 µl containing 1 µl of template DNA, 10 µl of PowerUp™ SYBR™ Green Master Mix (2X), 125 nM of *pir*A primers (Set 1, Set 2 and Set3), 150 nM of *pir*B primers (Set 1, Set 2 and Set2), 75 nM of shrimp internal control primers (β-Actin, EF1-α, G3PD and 18S rRNA) and 350 nM of 16S rRNA bacterial internal control primers. The primer concentration was determined by testing each primer set with concentrations that ranged from 50 nM to 500 nM. Each primer set listed in Table 1 was tested with one shrimp internal control primer pair and the bacterial 16S rRNA internal control primers. The real-time PCR conditions consisted of a UDG activation at 50 °C for 2 min, denature and Dual-Lock ™ DNA polymerase activation at 95 °C for 2 min, followed by 40 cycles at 95 °C for 3s and 59 °C for 30s. Following amplification, the melt curve analysis was performed. The reaction temperature was increased to 95 °C for 15s, then decreased to 60 °C for 1 min, and increased to 95 °C at a rate 0.1 °C per second with a continuous fluorescence monitoring. The melt curves were used to determine if the primers were compatible and primer combinations that showed four clear specific amplification peaks were considered adequate for the multiplex real-time PCR.

2.3. TaqMan probe design and duplex real-time PCR

TaqMan probes were designed for primer pair *pir*A F1/R1 and *pir*B F1/R1 using Geneious R11 [16]. The TaqMan probe for *pir*A F1/R1 (5′-GAACCAAACGGAGGCGTCA-3′) was synthesized and labeled with 6-Carboxy-4′,5′-Dichloro-2′, 7′-Dimethoxyfluorescein, Succinimidyl Ester (JOE) on the 5′ end and N, N, N′, N′-Tetramethyl-6-carboxyrhodamine (TAMARA) on the 3′ end. The TaqMan probe for *pir*B F1/R1 (5′- TCA CCTGCTGTTGGTTTTCCT-3′) was synthesized and labeled with 6-carboxyfluorescein (FAM) on the 5′ end and TAMARA on the 3′-end. For the assay, TaqMan™ Fast Virus 1-Step Master Mix (Applied Biosystems ™) was used, the final concentration for each primer was 0.2 µM and 0.07 µM for the TaqMan probe at a final volume of 10 µl. The real-time PCR profile was 20 s at 95 °C followed by 40 cycles of 1 s at 95 °C and 20 s at 59 °C. The amplification, detection and the analysis of the data for the real-time PCR assay was carried out with a StepOnePlus PCR system (Applied Biosystems ™).

2.4. Detection of the pirA and pirB genes in Vibrio spp.

Three natural known mutant strains of *V. parahaemolyticus* (*pir*A and partial *pir*B deletion), three strains of AHPND causing *V. campbelli*, one strain of *V. shiloi* (*pir*A positive and *pir*B negative) and ten strains of AHPND causing *V. parahaemolyticus* were obtained from the Aquaculture Pathology Laboratory bacterial collection. These bacteria were originally isolated from either the gastrointestinal tract of diseased shrimp, water or sediments from AHPND-affected farms in Asia or Latin America during 2013–2018. As negative controls three strains of *V. parahaemolyticus* without the *pir*A and *pir*B genes were used. These *Vibrio* spp. isolates were used to test the *pir*A, *pir*B and internal control primers (18S rRNA and 16S rRNA) for the SYBR Green and the TaqMan real-time PCR assays. All the tested strains were run by triplicate and the mean Ct values and melting temperatures were calculated. The DNA from the bacteria was extracted using the NORGEN Biotek Bacterial Genomic DNA isolation kit following the manufacturer's instructions.

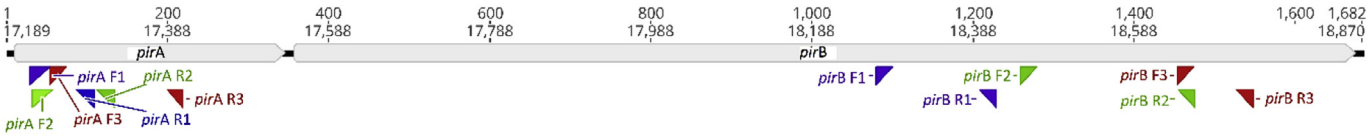

Fig. 1. The *pir*A and *pir*B primer locations on the virulence plasmid in the reference strain *Vibrio parahaemolyticus* A3. The primers *pir*A F1, *pir*A R1, *pir*B F1 and *pir*B R1 for dual detection of the *pir*A and *pir*B genes are shown in blue. The primers *pir*A F2, *pir*A R2, *pir*B F2 and *pir*B R2 for dual detection of the *pir*A and *pir*B genes are shown in green. The primers *pir*A F3, *pir*A R3, *pir*B F3 and *pir*B R3 for dual detection of the *pir*A and *pir*B genes are shown in red. The *pir*B primers are located near the 3′ end of the *pir*B gene allowing the detection of mutants with a partial deletion of *pir*B.

Table 2
A list of the internal control primers used in the SYBR Green assay for the amplification of *Photorhabdus* Insect-related (Pir) toxin genes *pir*A and *pir*B. For each primer, the nucleotide sequence, the Tm, the product size and the reference is shown. The genes used as internal controls were: β-Actin, Elongation factor1-alpha (EF1-α), Glyceroldehyde-3 phosphate dehydrogenase (GAPDH), 18S rRNA, and 16S rRNA.

Gene	Primer pair	Primer sequence (5′ to 3′)	Primer Tm	Product size (bp)	Reference
β-Actin	178F	GGTCGGTATGGGTCAGAAGGA	56	51	[17]
	228R	TTGCTTTGGGCCTCATCAC	59		
EF1-α	123F	TCGCCGAACTGCTGACCAAGA	51	55	[17]
	123R	CCGGCTTCCAGTTCCTTACC	51		
GAPDH	72F	CGTTGGACACCACCTTCA	59	55	[17]
	126R	GTGTGCGGTGTCAACATGGA	55		
18S rRNA	185F	ACCTGAGGCATCACAAGGGTTAT	48	61	[17]
	185R	GCTTGGTGTGCAATGTATTAACCTA	40		
16S rRNA	16S-rRNAF	TCCTACGGGAGGCAGCAGT	59.4	466	[18]
	16S-rRNAR	GGACTACCAGGGTATCTAATCCTGTT	58.1		
18S rRNA Set1	18S rRNAF1	GAGAGGGAGCCTGAGAAACG	59.8	72	This study
	18S rRNA R1	GTGCCGGGAGTGGGTAATTT	60.3		
18S rRNA Set 2	18S rRNA F1	TTTGAGTTCCGGGGGAAGTA	58.1	72	This study
	18S rRNA R1	ACTCCTGGTGGTGCCCTTC	61.5		

2.5. Experimental challenge of Penaeus vannamei with AHPND causing Vibrio parahaemolyticus

Specific Pathogen Free (SPF) *Penaeus vannamei* shrimp (average weight 1.0 g) were experimentally challenged via immersion following a previously published protocol [14]. Briefly, *V. parahaemolyticus* (Strain 13–028A/3) was grown in Tryptic Soy Broth containing 2% NaCl (TSB +) and incubated for 18 h before using for an immersion challenge (CFU 10^6/ml). The hepatopancreas was dissected out from the moribund animals and recently deceased animals, and it was used for detecting the pathogen via real-time PCR assays. The DNA from the hepatopancreas was extracted using Maxwell-16® Cell LEV DNA purification kit (Promega).

2.6. Specificity test

To verify there was no cross reactivity with other shrimp pathogens, the multiplex SYBR Green and the duplex TaqMan assays were tested using genomic DNA isolated from *P. vannamei* known to be infected with white spot syndrome virus (WSSV), *Enterocytozoon hepatopenaei* (EHP), infectious hypodermal and hematopoietic necrosis virus (IHHNV), necrotizing hepatopancreatic bacteria (NHPB), hepatopancreatic parvovirus (HPV), monodon baculovirus (MBV) and baculovirus penaei (BP).

2.7. Cloning of pirA and pirB amplicons

The DNA fragments for the *pir*A (80 bp) and *pir*B (149 bp) were amplified from *V. parahaemolyticus* 18–408 and cloned into the pDrive Cloning Vector (QIAGEN®). The plasmids were designated as *Vppir*A80 and *Vppir*B149. The plasmids were purified using QIAprep® Spin Miniprep Kit. The sequence of the *pir*A and *pir*B fragments was verified by sequencing at the sequencing facility of The University of Arizona, Tucson, AZ.

2.8. Sensitivity

The sensitivity of the SYBR Green and TaqMan real-time PCR assays were determined using 6-fold serial dilutions of purified *Vppir*A80 and *Vppir*B149 plasmids. The concentrations of plasmid DNA that were utilized ranged from 10^6 to 10^1 copies/μl for all the plasmids. Additionally, ten-fold serial dilutions of 20 ng/μl of total genomic DNA extracted from shrimp hepatopancreas (infected with reference strain A3) were used to determine the detection limit of both the SYBR Green and TaqMan PCR assays. All samples were tested in triplicates.

3. Results

3.1. Multiplex SYBR Green real-time PCR

Three sets of primers listed in Table 1 were tested for compatibility against the internal control primers listed in Table 2. Only primer set 1 and the internal controls 18S rRNA set 1 and 16S rRNA showed 4 distinguishable melt peaks corresponding to each amplified fragment (Fig. 2A). The amplicons for *pir*A, *pir*B, 18S rRNA and 16S rRNA from AHPND-infected shrimp showed easily distinguishable melting temperatures of 78.21 ± 0.18, 75.20 ± 0.20, 82.28 ± 0.34 and 85.41 ± 0.21 °C, respectively (Fig. 2).

3.2. Detecting the pirA and pirB genes in deletion mutants of Vibrio spp.

The real-time PCR results for different strains of bacteria are summarized in Table 3. The mean Ct and mean melting temperature are shown in Table 4. When a *Vibrio* sp. contained both the *pir*A and *pir*B genes or one of the two genes, a unique melting curve with unique peak (s) was produced. The *pir*A negative *V. parahaemolyticus* strains showed two amplicons, *pir*B and 16S rRNA, with melting temperatures of 75.20 ± 0.20 and 85.41 ± 0.21 °C, respectively (Fig. 2B). Similarly, the *pir*B negative strain showed two amplicons, *pir*A and 16S rRNA, with melting temperatures of 78.21 ± 0.18 and 85.41 ± 0.21 °C, respectively (Fig. 2C). The AHPND causing strains showed three amplicons, *pir*A, *pir*B and 16S rRNA, with melting temperatures of 78.21 ± 0.18, 75.20 ± 0.20 and 85.41 ± 0.21 °C, respectively (Fig. 2D).

The duplex TaqMan assay was also able to detect and differentiate when *Vibrio* spp. contained either *pir*A or *pir*B or both *pir*A and *pir*B. When *Vibrio* spp. contained both genes unique amplification curves were detected simultaneously in filter 1 (FAM/*pir*B) and filter 2 (JOE/*pir*A) (Fig. 3). In contrast, strains that contained only one gene showed a single amplification curve in filter 1 (FAM/*pir*B) or filter 2 (JOE/*pir*A) (Fig. 3). The results for the TaqMan assay for the different strains of bacteria are shown in Table 3. The SYBR Green assay and the TaqMan assay showed 100% agreement in the results for the detection of the *pir*A and *pir*B genes in the axenic *Vibrio* cultures and the hepatopancreas samples derived from AHPND-infected shrimp (N = 30). Both SYBR Green and TaqMan assays detected *pir*A and *pir*B genes in all the samples tested (Table 3). In Supplementary Fig. 1-3. the melt curves for each *Vibrio* spp. is presented.

3.3. Sensitivity

The lower limit of detection of the SYBR Green assay and the

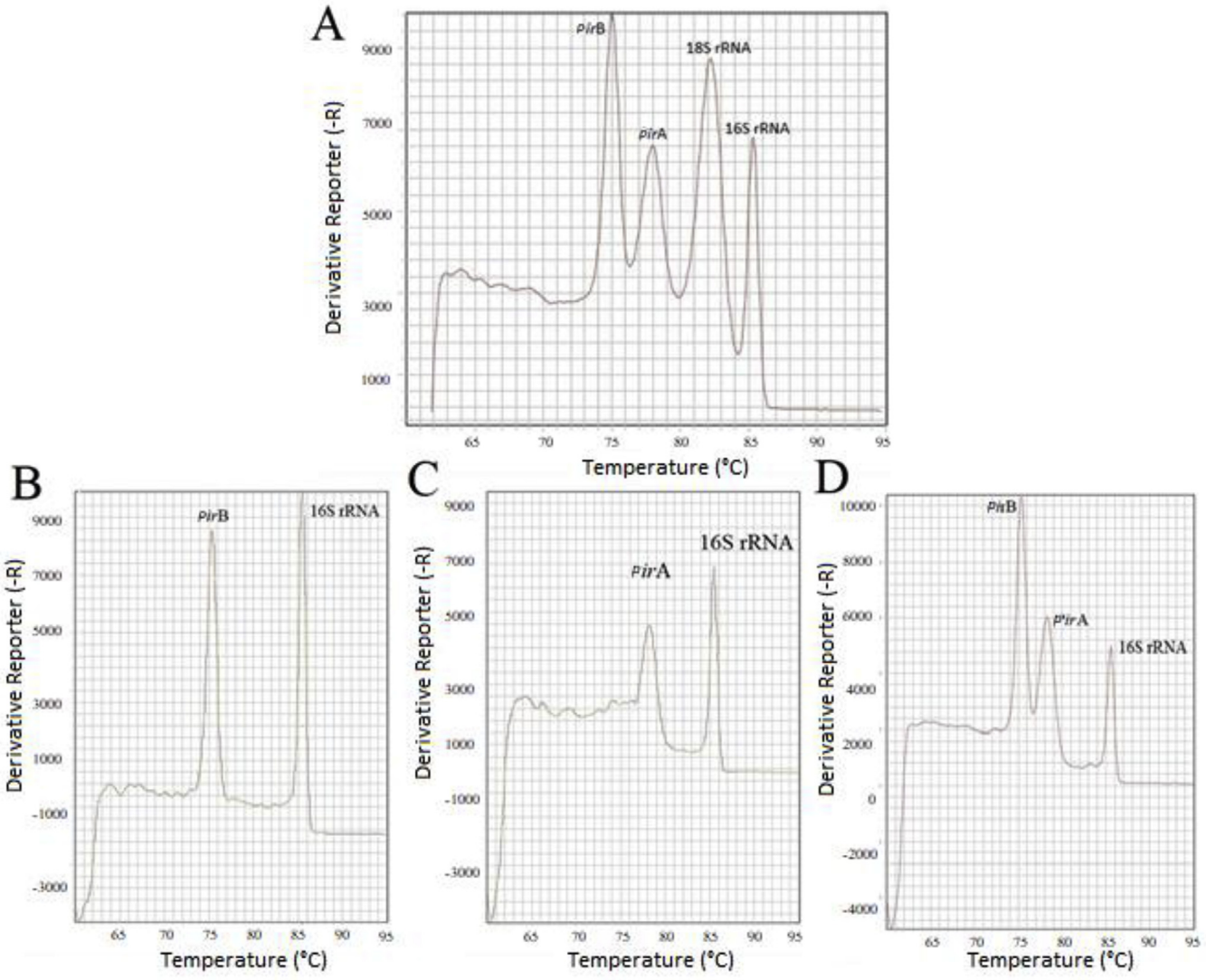

Fig. 2. Melt curve analysis of PCR amplicons derived from AHPND-infected shrimp tissue and *Vibrio* spp. (A) Melt curve analysis of infected shrimp tissue for *pir*A, *pir*B, 18S rRNA and 16S rRNA, the amplicons presented melting temperatures of 78.21 ± 0.18, 75.20 ± 0.20, 82.28 ± 0.34 and 85.41 ± 0.21 °C, respectively. (B) Melt curve analysis of *V. parahaemolyticus pir*A negative strain. The melting temperatures of *pir*B and 16S rRNA are 75.20 ± 0.20 and 85.41 ± 0.21 °C respectively. Each amplicon shows a clearly defined peak. (C) Melt curve pattern of *V. shiloi pir*B negative strain. The melting temperatures of *pir*A and 16S rRNA are 78.21 ± 0.18 and 85.41 ± 0.21 °C respectively. In (D) we can observe the melt curve analysis of AHPND-causing strains of *Vibrio* spp. The melting temperatures of *pir*A, *pir*B and 16S rRNA are 78.21 ± 0.18, 75.20 ± 0.20 and 85.41 ± 0.21 °C respectively. In A, B, C and D each amplicon shows a clearly defined peak.

Table 3
A summary of the results for the detection of the *pir*A, *pir*B, 18S rRNA and 16S rRNA genes by the multiplex SYBR Green real-time PCR and the duplex TaqMan |real-time PCR.

Strain	Species	*pir*A		*Pir*B		18S rRNA	16S rRNA
		SYBR	TaqMan	SYBR	TaqMan		
DA 16-250-8	*V. parahaemolyticus pir*A negative	Neg	Neg	Pos	Pos	Neg	Pos
D 16-250-9	*V. parahaemolyticus pir*A negative	Neg	Neg	Pos	Pos	Neg	Pos
DB 16-250	*V. parahaemolyticus pir*A negative	Neg	Neg	Pos	Pos	Neg	Pos
	V. shiloi	Pos	Pos	Neg	Neg	Neg	Pos
D 16-192	*V. campbelli* AHPND	Pos	Pos	Pos	Pos	Neg	Pos
D3 16-137	*V. campbelli* AHPND	Pos	Pos	Pos	Pos	Neg	Pos
D 52 B	*V. campbelli* AHPND	Pos	Pos	Pos	Pos	Neg	Pos
	V. parahaemolyticus AHPND (N = 9)	Pos	Pos	Pos	Pos	Neg	Pos
13–028 A3	AHPND Reference strain	Pos	Pos	Pos	Pos	Neg	Pos
B24-38	*V. parahaemolyticus* AHPND negative	Neg	Neg	Neg	Neg	Neg	Pos
B29-43	*V. parahaemolyticus* AHPND negative	Neg	Neg	Neg	Neg	Neg	Pos
C24-78	*V. parahaemolyticus* AHPND negative	Neg	Neg	Neg	Neg	Neg	Pos
Hepatopancreas tissue from *Penaeus vannamei shrimp* (N = 30)	Laboratory challenge test	Pos	Pos	Pos	Pos	Pos	Pos

Table 4
Mean Ct and melt temperatures of the different strains of *Vibrio* spp. and five samples of infected tissue. The table shows the mean and standard deviation of the Ct for the different strains of *Vibrio* spp. and five samples of infected tissue using the SYBR Green and TaqMan assays. For the TaqMan assay the Ct of the *pir*A and *pir*B amplicons is shown. Additionally, the mean and standard deviation of the melt temperatures (Tm) of the *pir*A, *pir*B, 18S rRNA and 16S rRNA amplicons is shown for all the *Vibrio* spp. and five samples of infected tissue.

Strain	Species	Mean Ct SYBR Green	Mean Ct TaqMan *pir*A	Mean Ct TaqMan *pir*B	Mean Tm *pir*A	Mean Tm *pir*B	Mean Tm 18S rRNA	Mean Tm 16S rRNA
DA 16-250-8	*V. parahaemolyticus pir*A negative	11.24 ± 0.63	-	12.97 ± 0.06		75.66 ± 0.17		85.74 ± 0.10
D 16-250-9	*V. parahaemolyticus pir*A negative	11.64 ± 0.33		12.26 ± 0.26		75.08 ± 0.05		85.56 ± 0.22
DB 16-250	*V. parahaemolyticus pir*A negative	14.69 ± 0.16		15.28 ± 0.01		75.27 ± 0.10		85.54 ± 0.086
	V. shiloi pirB negative	11.21 ± .59	12.42 ± 0.23		78.59 ± 0.38			85.62 ± 0.11
D 16-192	*V. campbelli* AHPND	12.48 ± 0.53	10.11 ± 0.04	9.81 ± 0.25	78.20 ± 20	75.21 ± 0.08		85.49 ± 0.08
D3 16-137	*V. campbelli* AHPND	10.52 ± 0.49	8.20 ± 0.11	8.25 ± 0.09	78.25 ± 0.22	75.29 ± 0.22		85.45 ± 0.25
D 52 B	*V. campbelli* AHPND	11.02 ± 0.39	16.19 ± 0.38	13.39 ± 0.11	78.21 ± 0.15	75.41 ± 0.07		85.57 ± 0.14
	V. parahaemolyticus AHPND	12. ± 0.19	11.81 ± 22	10.25 ± 0.05	78.20 ± 0.11	75.11 ± 0.01		85.44 ± 0.17
13–028 A3	AHPND Reference strain	15.05 ± 0.57	10.83 ± 0.07	10.92 ± 0.12	78.06 ± 0.6	75.10 ± 0.04		85.44 ± 0.84
B24-38	*V. parahaemolyticus* AHPND negative	9.75 ± 0.12						85.42 ± 0.02
B29-43	*V. parahaemolyticus* AHPND negative	10.75 ± 0.19						85.39 ± 0.10
C24-78	*V. parahaemolyticus* AHPND negative	9.33 ± 0.10						85.37 ± 0.07
1-Hepatopancreas from infected *P. vannamei*	Laboratory challenge test	23.14 ± 0.45	19.72 ± 0.22	20.03 ± 0.26	78.11 ± 0.28	75.10 ± 0.24	82.02 ± 0.06	85.40 ± 0.29
2- Hepatopancreas from infected *P. vannamei*	Laboratory challenge test	20.53 ± 0.42	17.30 ± 0.23	17.03 ± 0.15	78.18 ± 0.26	75.12 ± 0.27	82.00 ± 0.06	85.53 ± 0.23
3- Hepatopancreas from infected *P. vannamei*	Laboratory challenge test	19.36 ± 0.88	16.84 ± 0.21	16.69 ± 0.33	78.09 ± 0.25	75.11 ± 0.23	82.01 ± 0.06	85.42 ± 0.23
4- Hepatopancreas from infected *P. vannamei*	Laboratory challenge test	22.03 ± 0.58	18.07 ± 0.05	18.41 ± 0.03	78.09 ± 0.23	75.15 ± 0.20	82.32 ± 0.12	85.38 ± 0.48
5- Hepatopancreas from infected *P. vannamei*	Laboratory challenge test	28.26 ± 0.17	24.35 ± 0.07	25.86 ± 0.03	78.13 ± 0.09	75.12 ± 0.04	82.05 ± 0.10	85.35 ± 0.47

TaqMan assay for the *pir*A and *pir*B amplicons was 10 and 10 copies of recombinant plasmid containing these gene fragments (Fig. 4). Furthermore, the limit of detection for the *pir*A and *pir*B genes in infected shrimp hepatopancreas tissue for both assays was 200 fg of total DNA (Fig. 5). In Supplementary Fig 4. the melt curves of the serial dilution of DNA from infected tissue is shown. In Supplementary Fig 5. the detection limit (20 pg) of the conventional duplex PCR reported by Han et al. [11], is shown.

3.4. Specificity assay

In order to determine the specificity of SYBR Green and TaqMan assays described here, the methods were tested using DNA isolated from *P. vannamei* shrimp infected with several known viral (WSSV, IHHNV, HPV, MBV, BP), bacterial (NHPB) and fungal (EHP) pathogens. No amplification was obtained in the SYBR Green and TaqMan assays when DNA from other shrimp pathogens were used as a template indicating both assays are specific to *Vibrio* spp. that contain the *pir*A and *pir*B genes.

4. Discussion

Acute hepatopancreatic necrosis disease is caused by the *Vibrio* spp. that harbor a large plasmid with *Photorhabdus* Insect-Related (Pir) toxin genes *pir*A and *pir*B [11]. Both of these genes are necessary for virulence of the bacterium which can be highly lethal to cultured shrimp species of commercial importance. In this study, we developed a multiplex SYBR Green real-time PCR assay and a duplex TaqMan real-time PCR assay for the specific detection of the toxin genes *pir*A and *pir*B. The main advantage of both assays is the simultaneous detection and differentiation of the *pir*A and *pir*B genes, by utilizing the melt curve analysis for the SYBR Green assay and by using different reporter dyes for the TaqMan assay. To date, these are the only two real-time PCR assays published that can detect and simultaneously differentiate both genes in *Vibrio* spp.

Recently, Han et al. [3] and Kanrar & Dhar [15] reported the presence of mutant strains of *Vibrio* spp. that contained either the *pir*A or *pir*B gene. In AHPND-causing *Vibrio* spp., the binary toxin genes are flanked by transposes [11]. It has been proposed that due to a unique genome organization of the *V. parahaemolyticus* virulence plasmid, it may be lost or acquired by horizontal gene transfer via transposition or homologous recombination [2]. Further evidence of the transfer of these genes between bacteria is reported by Duran-Avelar et al. [10]. These authors detected the first non-*Vibrio* bacterium, *M. luteus,* that contains the *pir*A and *pir*B genes. It has not been reported if *M. luteus* is capable of causing AHPND. The discovery of several species of *Vibrio* and non-*Vibrio* bacteria carrying the binary toxin genes and causing AHPND suggest that there is an active transmission of the *pir*A and *pir*B genes between different bacteria and that these bacteria could acquire or lose pathogenicity. Therefore, the assays reported in this manuscript are fundamental tools for the study of plasmid transmission dynamics and for the detection of mutant strains that contain either *pir*A or *pir*B.

Multiplex SYBR Green real-time PCR using melt curve analysis has been previously used for the simultaneous detection of human pathogens (metapheumovirus, rhinovirus, enterovirus and coronavirus), plant pathogens (Plum pox virus), avian pathogens (avian influenza viruses) and bovine pathogens (*Clostridium botulinum*) [19–23]. The SYBR Green real-time PCR has been used for the detection and quantification of several shrimp pathogens including IHHNV, WSSV, TSV and YHV [24,25]. Considering the sensitivity and specificity of the SYBR Green assay when compared with the TaqMan assay and the low cost of the SYBR Green dyes, the method described here is a suitable tool for the detection of *Vibrio* spp. that cause AHPND and mutants strains that contain either the *pir*A or *pir*B gene. Furthermore, the SYBR Green assay described here has two internal controls (the shrimp 18S rRNA and the bacterial 16S rRNA) to avoid false negatives due to the

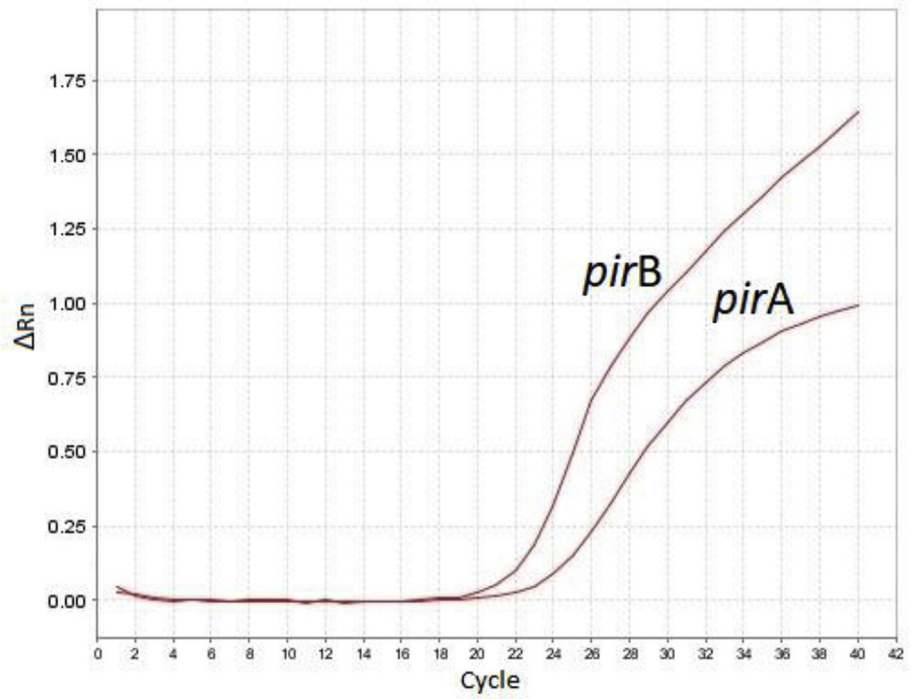

Fig. 3. Simultaneous amplification of the *pir*A and *pir*B genes by the duplex TaqMan assay. The amplification curves of *pir*A and *pir*B are indicated.

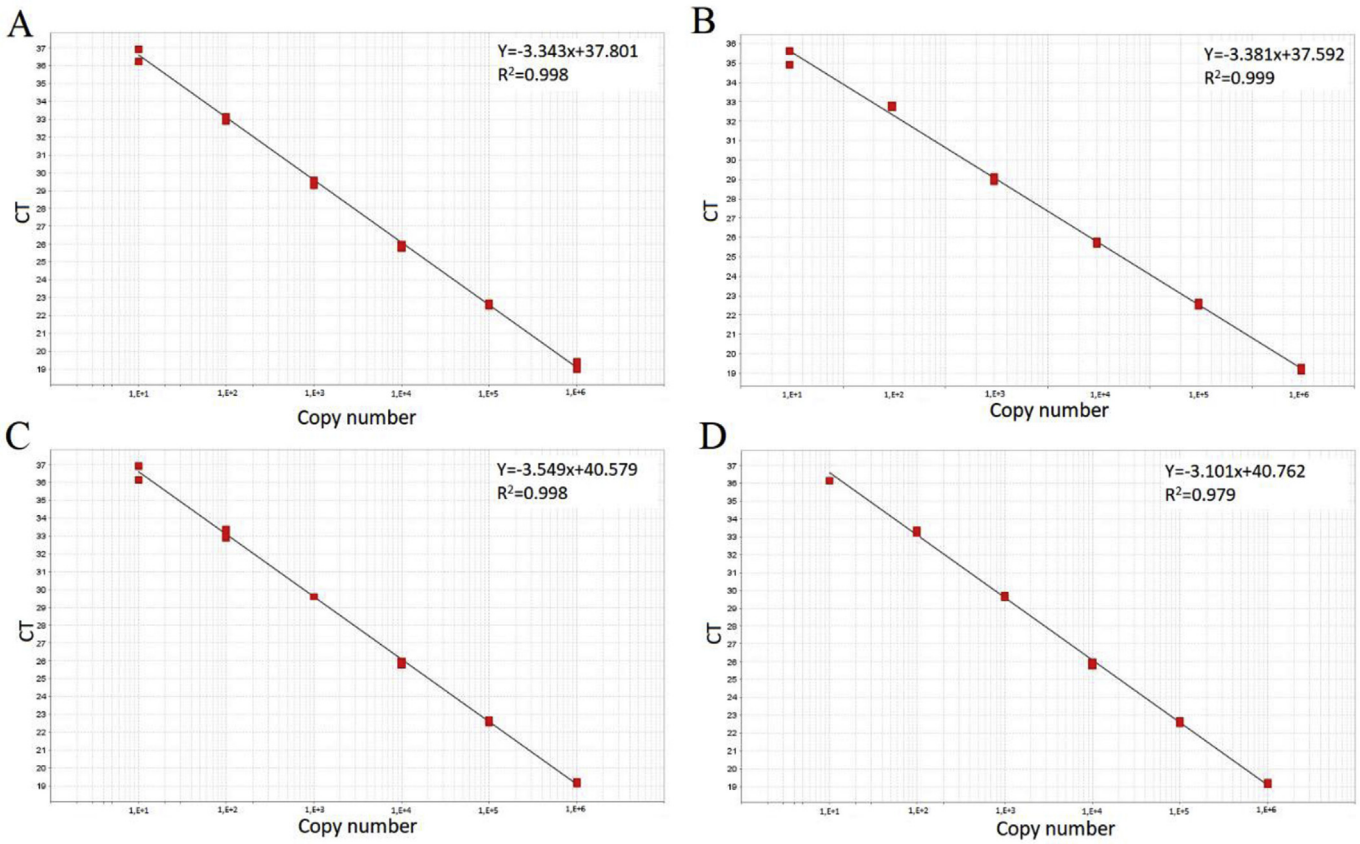

Fig. 4. Standard curve for the *pir*A and *pir*B genes. The *Vppir*A80 and *Vppir*B149 plasmids were serially diluted from 10^6 to 10^1 copies/μl and were used as a template for PCR. The Ct values are plotted against the logarithm of their respective copy number. (A) A standard curve for the *pir*A gene generated using the SYBR Green assay with a log linear dynamic range of 6 orders of magnitude with an R^2 value of 0.998, slope of −3.34 and amplification efficiency of 99.12%. (B) A standard curve for the *pir*B gene generated using the SYBR Green assay with a log linear dynamic range of 6 orders of magnitude with an R^2 value of 0.999, slope of −3.381 and amplification efficiency of 97.59%. (C) A standard curve for the *pir*A gene generated using the TaqMan assay with a log linear dynamic range of 6 orders of magnitude with an R^2 value of 0.998, slope of −3.549 and amplification efficiency of 91.32%. (D) A standard curve for the *pir*B gene generated using the TaqMan assay with a log linear dynamic range of 6 orders of magnitude with an R^2 value of 0.980, slope of −3.101 and amplification efficiency of 110.14%.

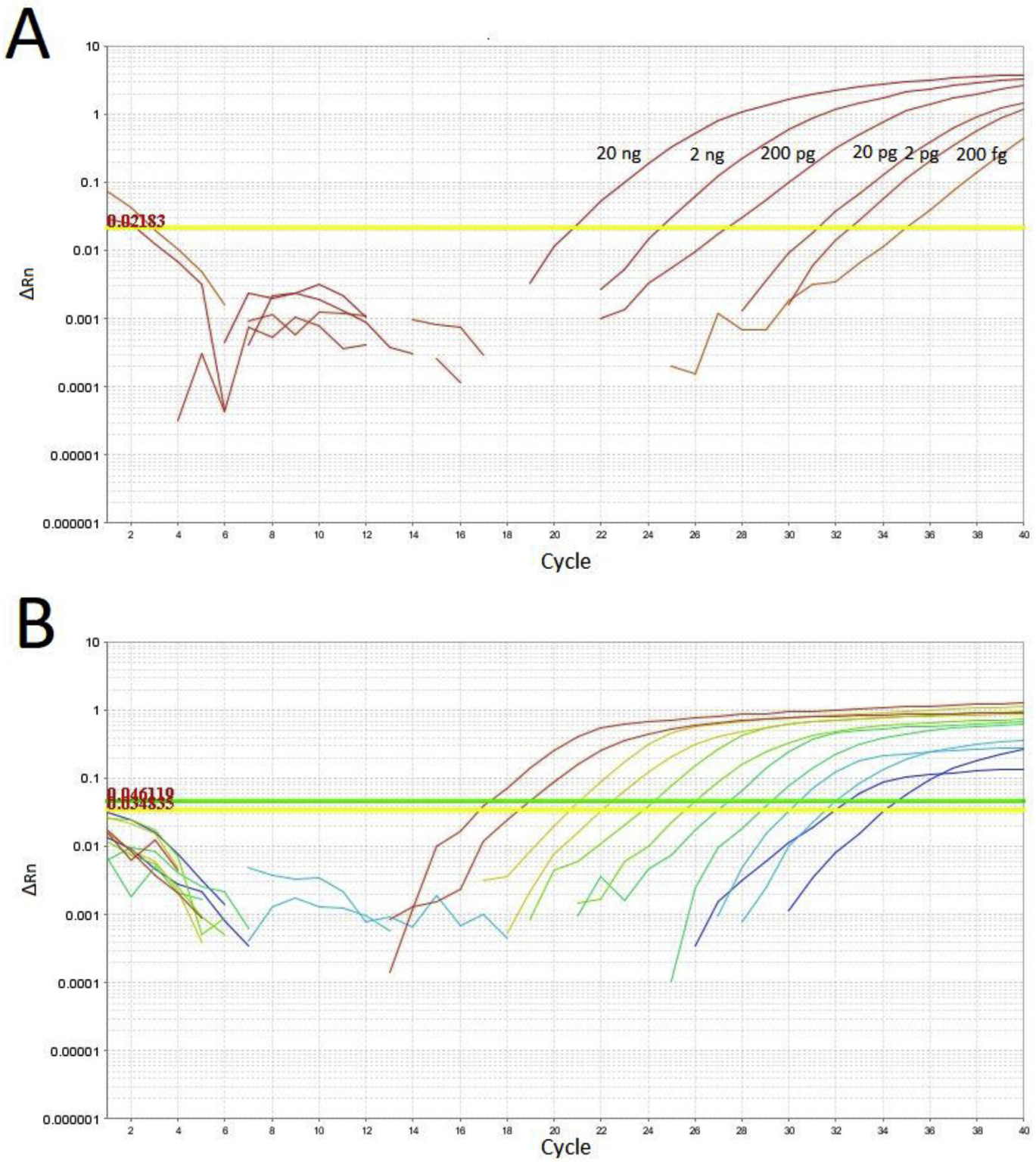

Fig. 5. Detection sensitivity of the SYBR Green and TaqMan assays using AHPND-infected *Penaeus vannamei* from the experimental challenge test. (A) The SYBR Green assay was able to detect the *pir*A, *pir*B, 18S rRNA and 16S rRNA down to 200 fg of total DNA. (B) The TaqMan assay showed a similar sensitivity also detecting both genes down to 200 fg of total DNA. The red amplification plot represents 20 ng of total DNA, *pir*A (Ct = 19.39 ± 0.44), *pir*B (Ct = 17.11 ± 0.23). The yellow amplification plot represents 2 ng of total DNA *pir*A (Ct = 22.80 ± 0.41), *pir*B (Ct = 20.53 ± 0.24). The green amplification plot represents 200 pg of total DNA *pir*A (Ct = 26.49 ± 0.15), *pir*B (Ct = 23 ± 0.27). The turquoise amplification plot represents 20 pg of total DNA *pir*A (Ct = 29.34 ± 0.26), *Pir*B (Ct = 27.19 ± 0.33). The light blue amplification plot represents 2 pg of total DNA *pir*A (Ct = 32.18 ± 12), *pir*B (Ct = 30.55 ± 0.27). The navy blue amplification plot represents 200 fg of total DNA *pir*A (Ct = 35.03 ± 0.32), *pir*B (Ct = 32.55 ± 0.30).

poor DNA quality or the inhibition during amplification. Based on the need, the assay can be performed in a single or duplex format for the detection of either one or both toxin genes. Duplex TaqMan real-time PCR has also been extensively used for the simultaneous detection of avian pathogens (avian reovirus and *Myoplasma synoviae*), human pathogens (*Eschrichia coli* O157), amphibian pathogens (*Batrachochytrium dendrobatidis* and *Batrachochytrium salamandrivorans*) and shrimp pathogens (WSSV, Taura Syndrome Virus and PstDNV1) [26–30]. The sensitivity and specificity of the TaqMan assay was equal to the SYBR Green assay and it can also be used in a single format to detect just one of the two toxin genes. An added advantage of the TaqMan assay is it requires much less time for completion (27 min) since no melt curve analysis is needed making this a valuable tool in detecting *Vibrio* spp. that causes AHPND as well as mutant strains. However, TaqMan assay is costlier than the SYBR Green assay due to the higher cost of the reagents and the probes.

To summarize, we have developed a multiplex SYBR Green and a duplex TaqMan real-time PCR for the simultaneous detection of the binary toxin genes, *pir*A and *pir*B, that are the virulence factors in causing AHPND in shrimp. The current OIE-recommended methods for AHPND detection is based on a one-step conventional PCR [3] and a nested PCR [13]. Therefore, the real-time PCR assays described here represent a valuable tool for detecting AHPND-causing *Vibrio* spp. The sensitivity and specificity of the assays will reduce time significantly compared to the current OIE-recommended methods.

Declaration of interest

None.

Authors' contributions

Roberto Cruz-Flores, Hung Nam Mai, Arun K. Dhar designed the experiments. Roberto Cruz-Flores wrote the manuscript, designed the primers and optimized the conditions of the multiplex SYBR Green real-time PCR and the duplex TaqMan real-time PCR. Roberto Cruz-Flores and Hung Nam Mai prepared the DNA samples. Hung Nam Mai prepared, maintained and extracted DNA from the axenic cultures of the different *Vibrio* spp. All authors reviewed and approved the final version of the manuscript.

Acknowledgements

Funding for this research was provided by the College of Agriculture & Life Sciences in The University of Arizona to Arun K. Dhar. This work was also partially supported by the USDA National Institute of Food and Agriculture, Animal Health project 1006512. The authors would like to thank Brenda Noble and Paul Schofield for performing an AHPND laboratory challenge and generating *P. vannamei* tissues.

Appendix A. Supplementary data

Supplementary data to this article can be found online at https://doi.org/10.1016/j.mcp.2018.12.004.

References

[1] L. Tran, L. Nunan, R. Redman, L. Mohney, C. Pantoja, K. Fitzsimmons, D. Lightner, Determination of the infectious nature of the agent of acute hepatopancreatic necrosis syndrome affecting penaeid shrimp, Dis. Aquat. Org. 105 (2013) 45–55, https://doi.org/10.3354/dao02621.

[2] C. Lee, I. Chen, Y. Yang, T. Ko, Y. Huang, J. Huang, M. Huang, S. Lin, C. Chen, S. Lin, V. Donald, H. Wang, A.H. Wang, H. Wang, L. Hor, C. Lo, Correction for Lee et al., the opportunistic marine pathogen Vibrio parahaemolyticus becomes virulent by acquiring a plasmid that expresses a deadly toxin, Proc. Natl. Acad. Sci. Unit. States Am. 112 (2015), https://doi.org/10.1073/pnas.1517100112 E5445–E5445.

[3] J.E. Han, K.F.J. Tang, L.F. Aranguren, P. Piamsomboon, Characterization and pathogenicity of acute hepatopancreatic necrosis disease natural mutants, pirABvp(-) V. parahaemolyticus, and pirABvp(+) V. campbellii strains, Aquaculture 470 (2017) 84–90, https://doi.org/10.1016/j.aquaculture.2016.12.022.

[4] L. Nunan, D. Lightner, C. Pantoja, S. Gomez-Jimenez, Detection of acute hepatopancreatic necrosis disease (AHPND) in Mexico, Dis. Aquat. Org. 111 (2014) 81–86, https://doi.org/10.3354/dao02776.

[5] FAO, Report of the FAO/MARD technical workshop on early mortality syndrome (EMS) or acute hepatopancreatic necrosis syndrome (AHPNS) of cultured shrimp (under TCP/VIE/3304), FAO fish, Aquac. Rep. 1053 (2013) 1–52.

[6] L. Liu, J. Xiao, M. Zhang, W. Zhu, X. Xia, X. Dai, Y. Pan, S. Yan, Y. Wang, A *Vibrio owensii* strain as the causative agent of AHPND in cultured shrimp, *Litopenaeus vannamei*, J. Invertebr. Pathol. 153 (2018) 156–164, https://doi.org/10.1016/j.jip.2018.02.005.

[7] X. Dong, H. Wang, G. Xie, P. Zou, C. Guo, Y. Liang, J. Huang, An isolate of *Vibrio campbellii* carrying the pir VP gene causes acute hepatopancreatic necrosis disease, Emerg. Microb. Infect. 6 (2017), https://doi.org/10.1038/emi.2016.131 e2–e2.

[8] H. Kondo, P.T. Van, L.T. Dang, I. Hirono, Draft genome sequence of non- *Vibrio parahaemolyticus* acute hepatopancreatic necrosis disease strain KC13.17.5, isolated from diseased shrimp in Vietnam, Genome Announc. 3 (2015) 2014–2015, https://doi.org/10.1128/genomeA.00978-15.

[9] L. Restrepo, B. Bayot, S. Arciniegas, L. Bajaña, I. Betancourt, F. Panchana, A. Reyes Muñoz, PirVP genes causing AHPND identified in a new Vibrio species (*Vibrio punensis*) within the commensal Orientalis clade, Sci. Rep. 8 (2018) 13080, https://doi.org/10.1038/s41598-018-30903-x.

[10] M. de J. Durán-Avelar, A. Vázquez-Reyes, A.L. González-Mercado, J.F. Zambrano-Zaragoza, M.F. Ayón-Pérez, J.M. Agraz-Cibrián, J. Gutiérrez-Franco, N. Vibanco-Pérez, Pir A- and pirB -like gene identification in Micrococcus luteus strains in Mexico, J. Fish. Dis. (2018) 1–7, https://doi.org/10.1111/jfd.12874.

[11] J. Han, K. Tang, L. Tran, D. Lightner, Photorhabdus insect-related (Pir) toxin-like genes in a plasmid of *Vibrio parahaemolyticus*, the causative agent of acute hepatopancreatic necrosis disease (AHPND) of shrimp, Dis. Aquat. Org. 113 (2015) 33–40, https://doi.org/10.3354/dao02830.

[12] Y.-T. Yang, I.-T. Chen, C.-T. Lee, C.-Y. Chen, S.-S. Lin, L. Hor, T.-C. Tseng, Y.-T. Huang, K. Sritunyalucksana, S. Thitamadee, H.-C. Wang, C.-F. Lo, Draft genome sequences of four strains of *Vibrio parahaemolyticus*, three of which cause early mortality syndrome/acute hepatopancreatic necrosis disease in shrimp in China and Thailand, Genome Announc. 2 (2014) 2–3, https://doi.org/10.1128/genomeA.00816-14.

[13] S. Dangtip, R. Sirikharin, P. Sanguanrut, S. Thitamadee, K. Sritunyalucksana, S. Taengchaiyaphum, R. Mavichak, P. Proespraiwong, T.W. Flegel, AP4 method for two-tube nested PCR detection of AHPND isolates of *Vibrio parahaemolyticus*, Aquac. Reports 2 (2015) 158–162, https://doi.org/10.1016/j.aqrep.2015.10.002.

[14] J.E. Han, K.F.J. Tang, C.R. Pantoja, B.L. White, D.V. Lightner, qPCR assay for detecting and quantifying a virulence plasmid in acute hepatopancreatic necrosis disease (ahpnd) due to pathogenic *vibrio parahaemolyticus*, Aquaculture 442 (2015) 12–15, https://doi.org/10.1016/j.aquaculture.2015.02.024.

[15] S. Kanrar, A.K. Dhar, Complete genome sequence of a deletion mutant of *Vibrio parahaemolyticus* from pacific white shrimp (*Penaeus vannamei*), Genome Announc. 6 (2018) 33–40, https://doi.org/10.1128/genomeA.00544-18.

[16] M. Kearse, R. Moir, A. Wilson, S. Stones-Havas, M. Cheung, S. Sturrock, S. Buxton, A. Cooper, S. Markowitz, C. Duran, T. Thierer, B. Ashton, P. Meintjes, A. Drummond, Geneious Basic: an integrated and extendable desktop software platform for the organization and analysis of sequence data, Bioinformatics 28 (2012) 1647–1649, https://doi.org/10.1093/bioinformatics/bts199.

[17] A.K. Dhar, R.M. Bowers, K.S. Licon, G. Veazey, B. Read, Validation of reference genes for quantitative measurement of immune gene expression in shrimp, Mol. Immunol. 46 (2009) 1688–1695, https://doi.org/10.1016/j.molimm.2009.02.020.

[18] M. Nadkarni, F.E. Martin, N.A. Jacques, N. Hunter, Determination of bacterial load by real-time PCR using a broad range (universal) probe and primer set, Microbiology 148 (2002) 257–266, https://doi.org/10.1128/JCM.40.5.1698.

[19] G. Boivin, P. De, G. De Serres, M.G. Bergeron, Multiplex real-time PCR assay for detection of influenza and human respiratory syncytial viruses, J. Clin. Microbiol. 42 (2004) 45–51, https://doi.org/10.1128/JCM.42.1.45–51.2004.

[20] A. Varga, D. James, Detection and differentiation of Plum pox virus using real-time multiplex PCR with SYBR Green and melting curve analysis: a rapid method for strain typing, J. Virol Methods 123 (2005) 213–220, https://doi.org/10.1016/j.jviromet.2004.10.005.

[21] W.T. Ong, A.R. Omar, A. Ideris, S.S. Hassan, Development of a multiplex real-time PCR assay using SYBR Green 1 chemistry for simultaneous detection and subtyping of H9N2 influenza virus type A, J. Virol Methods 144 (2007) 57–64, https://doi.org/10.1016/j.jviromet.2007.03.019.

[22] F. Anniballi, B. Auricchio, E. Delibato, M. Antonacci, D. De Medici, L. Fenicia, Multiplex real-time PCR SYBR Green for detection and typing of group III *Clostridium botulinum*, Vet. Microbiol. 154 (2012) 332–338, https://doi.org/10.1016/j.vetmic.2011.07.018.

[23] M. Sultani, T. Mokhtari Azad, M. Eshragian, A. Shadab, M. Naseri, O. Eilami, J. Yavarian, Multiplex SYBR green real-time PCR assay for detection of respiratory viruses, Jundishapur J. Microbiol. 8 (2015) 1–5, https://doi.org/10.5812/jjm.19041v2.

[24] A.K. Dhar, M.M. Roux, K.R. Klimpel, Detection and quantification of infectious hypodermal and hematopoietic necrosis virus and white spot virus in shrimp using real-time quantitative PCR and SYBR green chemistry, J. Clin. Microbiol. 39 (2001) 2835–2845, https://doi.org/10.1128/JCM.39.8.2835–2845.2001.

[25] A.K. Dhar, M.M. Roux, K.R. Klimpel, Quantitative assay for measuring the Taura syndrome virus and yellow head virus load in shrimp by real-time RT-PCR using SYBR Green chemistry, J. Virol Methods 104 (2002) 69–82, https://doi.org/10.1016/S0166-0934(02)00042-3.

[26] C. Hsu, T. Tsai, T. Pan, Use of the duplex TaqMan PCR system for detection of shiga-like toxin-producing *Escherichia coli* O157, Society 43 (2005) 2668–2673, https://doi.org/10.1128/JCM.43.6.2668.

[27] Z. Xie, L. Xie, Y. Pang, Z. Lu, Z. Xie, J. Sun, X. Deng, J. Liu, X. Tang, M. Khan, Development of a real-time multiplex PCR assay for detection of viral pathogens of penaeid shrimp, Arch. Virol. 153 (2008) 2245–2251, https://doi.org/10.1007/s00705-008-0253-0.

[28] M. Blooi, F. Pasmans, J.E. Longcore, A. Spitzen-Van Der Sluijs, F. Vercammen, A. Martel, Duplex real-Time PCR for rapid simultaneous detection of *Batrachochytrium dendrobatidis* and *Batrachochytrium salamandrivorans* in amphibian samples, J. Clin. Microbiol. 51 (2013) 4173–4177, https://doi.org/10.1128/JCM.02313-13.

[29] L. Huang, Z. Xie, L. Xie, X. Deng, Z. Xie, S. Luo, J. Huang, T. Zeng, J. Feng, A duplex real-time PCR assay for the detection and quantification of avian reovirus and *Mycoplasma synoviae*, Virol. J. 12 (2015) 1–9, https://doi.org/10.1186/s12985-015-0255-y.

[30] C.A.G. Leal, A.F. Carvalho, R.C. Leite, H.C.P. Figueiredo, Development of duplex real-time PCR for the detection of WSSV and PstDV1 in cultivated shrimp, BMC Vet. Res. 10 (2014) 2–7, https://doi.org/10.1186/1746-6148-10-150.